Phosphorothioate backbone modifications of nucleotide-based drugs are potent platelet activators

Article

Published February 2, 2015

Phosphorothioate backbone modifications of nucleotide-based drugs are potent platelet activators

Ulrike Flierl,[1,8] Tracy L. Nero,[2,3] Bock Lim,[1] Jane F. Arthur,[4] Yu Yao,[1] Stephanie M. Jung,[5] Eelo Gitz,[6] Alice Y. Pollitt,[6] Maria T.K. Zaldivia,[1] Martine Jandrot-Perrus,[7] Andreas Schäfer,[8] Bernhard Nieswandt,[9] Robert K. Andrews,[4] Michael W. Parker,[2,3] Elizabeth E. Gardiner,[4]* and Karlheinz Peter[1]*

[1]Baker IDI Heart and Diabetes Institute, [2]St. Vincent's Institute of Medical Research, and [3]Bio21 Institute, University of Melbourne, Melbourne, Victoria 3010, Australia
[4]Australian Centre for Blood Diseases, Monash University, Melbourne, Victoria 3004, Australia
[5]Department of Biochemistry, University of Cambridge, Cambridge CB2 1GA, England, UK
[6]Centre for Cardiovascular Sciences, University of Birmingham, Birmingham B15 2TT, England, UK
[7]Institut National de la Santé et de la Recherche Médicale, U1148, 75877 Paris, France
[8]Department of Cardiology and Angiology, Hannover Medical School, 30625 Hannover, Germany
[9]Rudolf Virchow Centre for Experimental Biomedicine, D-97080 Würzburg, Germany

Nucleotide-based drug candidates such as antisense oligonucleotides, aptamers, immunoreceptor-activating nucleotides, or (anti)microRNAs hold great therapeutic promise for many human diseases. Phosphorothioate (PS) backbone modification of nucleotide-based drugs is common practice to protect these promising drug candidates from rapid degradation by plasma and intracellular nucleases. Effects of the changes in physicochemical properties associated with PS modification on platelets have not been elucidated so far. Here we report the unexpected binding of PS-modified oligonucleotides to platelets eliciting strong platelet activation, signaling, reactive oxygen species generation, adhesion, spreading, aggregation, and thrombus formation in vitro and in vivo. Mechanistically, the platelet-specific receptor glycoprotein VI (GPVI) mediates these platelet-activating effects. Notably, platelets from GPVI function–deficient patients do not exhibit binding of PS-modified oligonucleotides, and platelet activation is fully abolished. Our data demonstrate a novel, unexpected, PS backbone–dependent, platelet-activating effect of nucleotide-based drug candidates mediated by GPVI. This unforeseen effect should be considered in the ongoing development programs for the broad range of upcoming and promising DNA/RNA therapeutics.

CORRESPONDENCE
Karlheinz Peter:
karlheinz.peter@bakeridi.edu.au

Abbreviations used: ADP, adenosine diphosphate; CBD, collagen-binding domain; CRP, collagen-related peptide; CRP-XL, cross-linked CRP; DIC, differential interference contrast; GPVI, glycoprotein VI; ITAM, immunoreceptor tyrosine-based activation motif; ODN, oligodeoxynucleotide; PMA, platelet-monocyte aggregate; PRP, platelet-rich plasma; PS, phosphorothioate; ROS, reactive oxygen species; RT, room temperature.

Platelets mediate hemostasis and are crucial for appropriate inflammatory and immune responses (Semple and Freedman, 2010). Platelets express several TLRs (Cognasse et al., 2005) including TLR9, which binds unmethylated bacterial and viral DNA (Iwasaki and Medzhitov, 2004). The discovery of immunostimulatory properties of specialized bacterial and mammalian DNA motifs that bind TLR9 (Hemmi et al., 2000) and regulate protective immune defense mechanisms has provided new options for prophylaxis and/or therapy for infectious, allergic, and malignant diseases (Krieg et al., 1995). Short single-stranded DNA molecules (oligonucleotides) were developed as potential drug candidates. To prevent these oligonucleotides from being rapidly degraded by cellular and/or plasma nucleases, phosphorothioate (PS) modification was used whereby nonbridging oxygen molecules are replaced with sulfur (Lennox and Behlke, 2011). We investigated the consequences of exposure of platelets to TLR9 agonists and other therapeutic oligonucleotides and discovered an unexpected, PS modification–dependent activation of platelets

*E.E. Gardiner and K. Peter contributed equally to this paper.

The Rockefeller University Press $30.00
J. Exp. Med. 2015 Vol. 212 No. 2 129–137
www.jem.org/cgi/doi/10.1084/jem.20140391

Published February 2, 2015

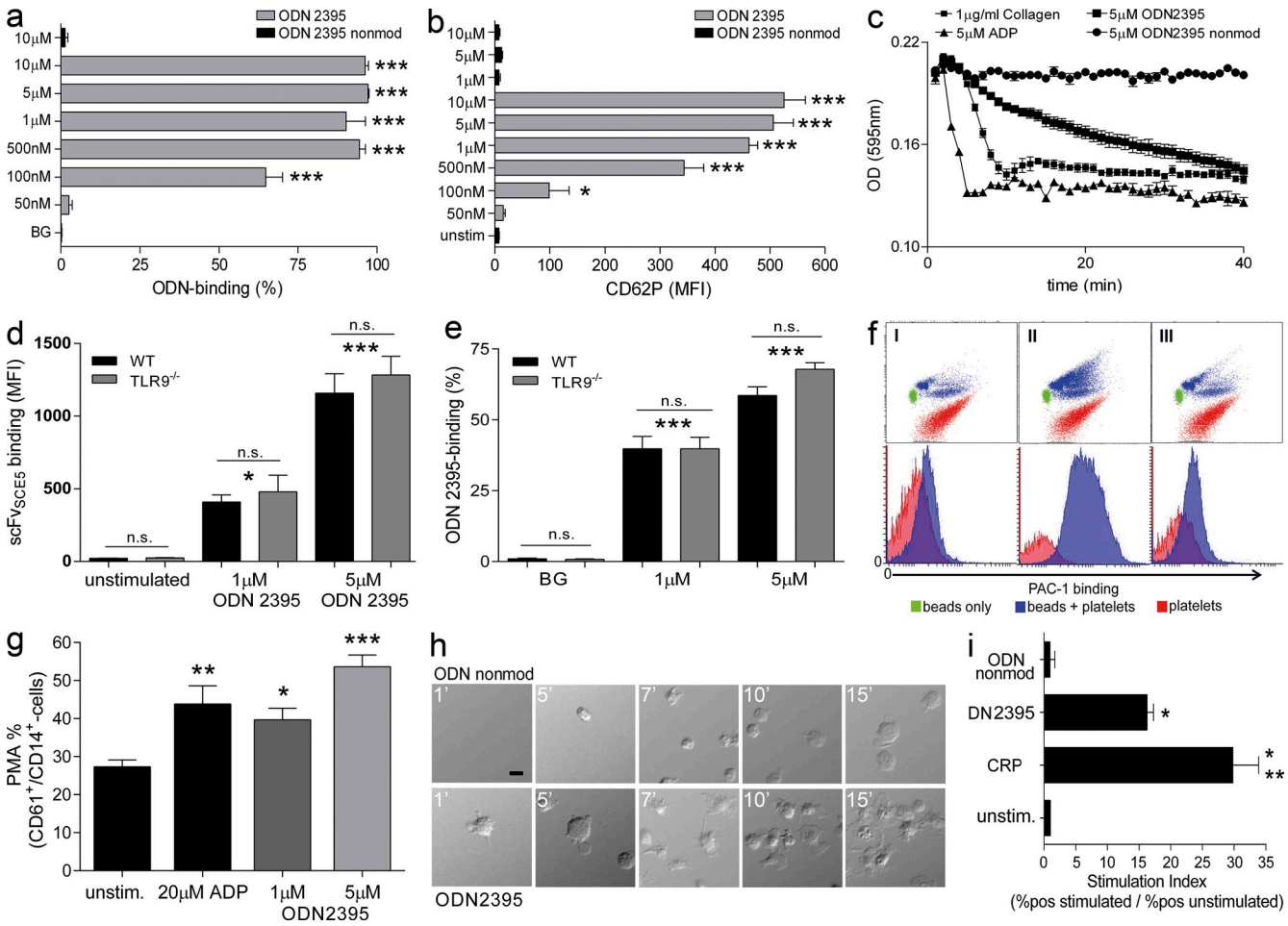

Figure 1. ODN2395 binding to platelets and induction of platelet activation, aggregation, and adhesion. (a) ODN2395 was incubated with platelets and binding was assessed (***, P < 0.001 vs. background [BG], 10 µM non–PS-modified ODN2395 ["ODN2395 nonmod"], and 50 nM ODN2395; *n* = 6). (b) CD62P surface expression after ODN2395 incubation of human washed platelets compared with unstimulated control samples and ODN2395 nonmod (*, P < 0.05 vs. unstimulated/1–10 µM ODN2395 nonmod/50 nM ODN2395; ***, P < 0.001 vs. unstimulated/1–10 µM ODN2395 nonmod/50 nM ODN2395; *n* = 5). (c) Platelet aggregation after 5 µM ODN2395 stimulation of PRP; final aggregation compared with 5 µM ADP/1 µg/ml collagen stimulation; representative aggregation curves (*n* = 6). (d) Murine GPIIb/IIIa activation after incubation with ODN2395 (1 µM/5 µM; *, P < 0.05/***, P < 0.001 vs. unstimulated WT/TRL9$^{-/-}$; *n* = 4–5) detected on platelets from WT or mice deficient in TLR9 (TRL9$^{-/-}$) using a single chain antibody (scFv$_{SCE5}$), which binds to activated murine GPIIb/IIIa. (e) Binding of 1 or 5 µM ODN2395 to platelets from WT and TRL9$^{-/-}$ mice (1 µM/5 µM; ***, P < 0.001 vs. BG WT/TRL9$^{-/-}$; *n* = 4–5). (f) Coincubation of 1-µm streptavidin beads alone (I) or beads coated with ODN2395 (II) or ODN2395 nonmod (III) with human washed platelets assessed for binding and activation of platelets by ODN2395-coated beads; representative dot blots and histograms of four independently performed experiments are shown. (g) Whole blood incubation with ODN2395 on PMA formation (*, P < 0.05; **, P < 0.01; ***, P < 0.001 vs. unstimulated; *n* = 10). (h) DIC microscopy of washed human platelets adhering to 30 µg/ml fibrinogen-coated glass slides at the indicated time points; ODN2395 vs. nonmodified ODN2395 (labeled as ODN nonmod); shown is one representative experiment (*n* = 3). Bar, 2 µm. (i) Intraplatelet ROS production after treatment with 10 µg/ml CRP-XL (positive control), 5 µM ODN2395, or 5 µM ODN nonmod (*, P < 0.05 vs. unstim./ODN nonmod; **, P < 0.01 vs. ODN; *n* = 3). Data are presented as means ± SEM.

mediated by the platelet-specific collagen receptor glycoprotein VI (GPVI), a signaling/adhesion receptor with important roles in platelet function.

RESULTS AND DISCUSSION

PS backbone modification induces platelet activation

Incubation of the PS oligodeoxynucleotides (ODNs [ODN2395]) with human platelets demonstrated concentration-dependent binding (Fig. 1 a), platelet activation (P-selectin up-regulation; Fig. 1 b), and platelet aggregation (Fig. 1 c). In contrast, ODN2395 binding to leukocytes was low, with only CD14$^+$ cells demonstrating weak binding, which did not result in monocyte activation as assessed in flow cytometry using the single-chain antibody MAN-1, which binds selectively to the active conformation of integrin Mac-1 (not depicted; Eisenhardt et al., 2007). Unexpectedly, platelet activation was sequence (not depicted)- and TLR9-independent (Fig. 1, d and e) but required PS backbone modifications of oligonucleotides.

Published February 2, 2015

Oligonucleotides with a native phosphodiester backbone (ODN2395 nonmodified [nonmod]) did not bind (Fig. 1 a) or activate (Fig. 1 b) platelets. Platelets bound to ODN2395 immobilized on beads demonstrated significantly increased binding of the platelet activation–specific mAb PAC-1 (GPIIb/IIIa activation; Fig. 1 f). Elevated levels of platelet-monocyte aggregates (PMAs), reflecting clinically relevant platelet activation (Tapp et al., 2012), were significantly increased in whole blood when mixed with ODN2395 (Fig. 1 g) but not ODN2395 nonmod (not depicted). Treatment of human platelets with ODN2395 also resulted in more rapid adhesion and spreading on fibrinogen (Fig. 1 h) and production of reactive oxygen species (ROS), mirroring the effects typically seen for GPVI ligands (Fig. 1 i; Arthur et al., 2012).

PS substitution can alter RNA/DNA conformation, protein binding properties, and physicochemical properties (Krieg et al., 2003). Substitution of a nonbridging oxygen atom with a sulfur atom in the phosphodiester backbone introduces chirality around the phosphorus atom, and the number of diastereomers produced by this chirality is 2^n, where n is the number of PS links introduced (Eckstein, 2000). With 22 PS modifications, ODN2395 potentially contains 2^{22} (or 4,194,304) diastereomers. The sulfur atom has a larger van der Waal's radius (1.8 compared with 1.4 Å) and sulfur-phosphorus bond length (1.9 compared with 1.5 Å) than oxygen (Eckstein, 2000). The sulfur atom is less electronegative than oxygen (respectively, 2.5 and 3.5 on the Pauling scale), but the negative charge is more confined to the sulfur atom, making the PS ODN backbone more "polyanionic" than the native phosphodiester. The PS ODN sulfur can participate in strong hydrogen bonding with a longer bond length than the equivalent phosphodiester ODN. Together these physicochemical differences may permit specific binding of PS ODNs to cellular proteins.

PS modification causes receptor-mediated signaling in platelets

To assess the effects of ODN2395 on in vitro thrombus formation, anticoagulated whole blood was passed across collagen- or fibrinogen-coated microchannels. ODN2395, but not nonmod ODN2395, caused rapid and extensive thrombus formation (Fig. 2 a). As platelet-specific GPIbα of the GPIb-IX-V complex activates platelets when engaged by von Willebrand factor (VWF) under flow, we assessed a role for GPIbα in mediating ODN2395 effects. Washed platelets were treated with *Naja kaouthia* metalloprotease Nk, which specifically removes the N-terminal VWF-binding region of GPIbα. Untreated and Nk-treated platelets bound ODN2395 effectively and were activated to the same extent (Fig. 2, b and c), indicating that GPIbα is not involved in mediating ODN2395-induced activation.

Investigating the kinases Syk and Src allows us to draw conclusions about their upstream receptors, the so-called immunoreceptor tyrosine-based activation motif (ITAM) receptors. Human platelets express GPVI, C-type lectin-like receptor 2 (CLEC-2), and FcγRIIa, which signal through ITAMs. FcγRIIa is not present on mouse platelets (McKenzie et al., 1999). ODN2395-mediated platelet activation was significantly attenuated by platelet pretreatment with Src kinase inhibitor PP2 or Syk inhibitor BAY 61-3606 at concentrations previously shown to specifically block Src and Syk activity in platelets (Fig. 2 d; Hu et al., 2011). Moreover, rapid tyrosine phosphorylation of the GPVI-associated FcRγ chain and several other intracellular proteins occurs upon GPVI cross-linking by collagen (Gibbins et al., 1996). Lysates of ODN2395-treated platelets exhibited significant phosphorylation of Syk and Src kinases, resembling the extent of phosphorylation observed in lysates treated with cross-linked collagen-related peptide (CRP [CRP-XL]), a GPVI-specific agonist (Fig. 2 e). ODN2395-dependent phosphorylation of Syk and Src was further confirmed by immunoprecipitation of phosphorylated tyrosine proteins and specific Western blots for these kinases (not depicted). Protein phosphorylation events induced by ODN2395 were delayed (~5 min) compared with CRP-XL–induced tyrosine phosphorylation, consistent with the observed delayed response in ODN2395-induced platelet aggregation (Fig. 1 c), as GPVI clustering and oligomerization is essential to elicit a full GPVI signaling response and platelet activation. This delayed response is likely to reflect the ability of ODN2395 to affect receptor clustering, an outcome which will be influenced by the affinity/avidity and kinetics of PS ODN binding to GPVI, the extent of PS ODN oligomerization, and donor-variable GPVI surface density.

Collectively, the platelet counter-receptor for PS ODNs was likely to be an ITAM signaling receptor, most probably GPVI. This hypothesis was substantiated by the binding of a dimeric GPVI-Fc construct incorporating amino acids 1–236 of human GPVI to immobilized ODN2395 (Fig. 2 f; Grüner et al., 2005). Pull-down experiments using GPVI-Fc and beads coated with PS-modified or nonmodified ODN2395 confirmed GPVI as a specific binding partner for PS ODNs (Fig. 2 g).

GPVI is a receptor for PS-modified ODNs

To further define the role of GPVI as a receptor that mediates ODN2395 activity, we used the unique opportunity to obtain blood from patients with GPVI deficiency. Blood of two patients without medication, with mild bleeding symptoms, normal platelet counts, and normal response to adenosine diphosphate (ADP) and ristocetin but not collagen or CRP-XL in platelet aggregometry, was investigated (not depicted). Flow cytometry revealed normal platelet surface levels of GPIbα and integrin αIIb, but only 10% of levels of GPVI measured in a healthy donor analyzed on the same day (not depicted). Patient platelet lysates contained normal amounts of ITAM-containing CLEC-2 as detected by Western blot (not depicted). Platelet-rich plasma (PRP) from GPVI-deficient patients did not support ODN2395/platelet binding or activation even at oligonucleotide concentrations up to 10 μM (Fig. 2 h), strongly suggesting that GPVI is a platelet receptor for ODN2395. Consistent with this are our findings that pretreatment of healthy

Published February 2, 2015

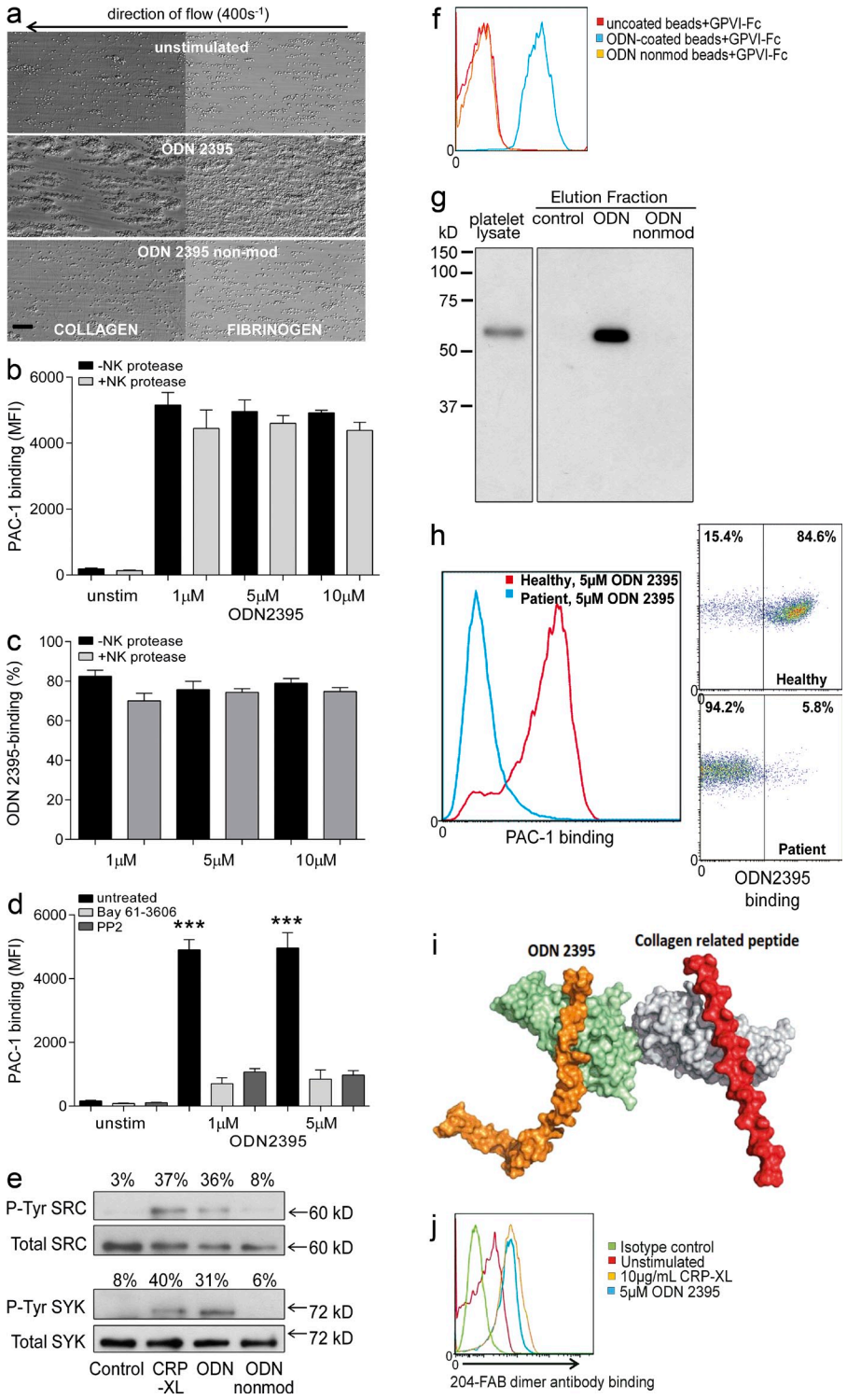

Figure 2. ODN2395–induced signaling and GPVI as target receptor of PS oligonucleotides. (a) Platelet adhesion and thrombus formation under flow conditions after ODN2395 preincubation: collagen coating (100 µg/ml; left), fibrinogen coating (100 µg/ml; right), untreated control (top), 5 µM ODN2395 (middle), and 5 µM ODN2395 nonmod (bottom; $n = 3$). Bar, 50 µm. (b and c) Platelet activation/binding of ODN2395 after preincubation with Nk protease ($n = 4$). (d) Impact of Syk kinase inhibitor Bay 61-3606 (5 µM) and the Src kinase inhibitor PP2 (5 µM) on further downstream signaling (***, $P < 0.001$ vs. preincubated sample with Syk/Src kinase inhibitors; $n = 4–5$). (e) Phosphorylation of Syk/Src after PS ODN incubation (5 µM) of platelets compared with control and ODN nonmod–incubated samples; 5 µg/ml CRP-XL served as positive control (shown is one representative experiment; $n = 4$). (f) Binding of GPVI fusion construct (GPVI-Fc) to ODN2395-coated beads compared with uncoated/ODN nonmod–coated beads; a recombinant human ICAM-1 Fc chimera, which shares ectodomain conformational similarities with GPVI, served as a control (shown is one representative histogram; $n = 3$). (g) Pull-down assays identified GPVI as a binding partner for ODN2395; representative Western blot detecting GPVI ($n = 2$). (h) Extent of platelet activation (histogram) and ODN2395 binding (dot blots) to human GPVI-deficient platelets (shown are representative histograms/dot blots obtained from two GPVI-deficient patients). (i) Crystal structure of the GPVI CBD dimer and putative interactions with ODN2395 (orange)/CRP (red). (j) 5 µM ODN2395–induced GPVI dimer formation detected by binding of an anti-GPVI dimer-specific Fab (204-FAB; shown is one representative experiment; $n = 3$). Data are presented as means ± SEM.

donor platelets with function-blocking antibodies against human CLEC-2 or CD36 did not ablate ODN2395 binding or activation of platelets; however, pretreatment with the function-blocking anti-GPVI antibody (9012.2; Mangin et al., 2012) prevented ODN2395-induced platelet aggregation (not depicted).

A site-directed mutagenesis study has identified residues in the GPVI collagen-binding domain (CBD) that are involved with collagen or CRP binding (Horii et al., 2006). These residues are located in a groove on domain D1 of each monomer in the CBD; this groove is lined by basic residues, is electropositive, and would be an ideal site for the anionic (negatively

Published February 2, 2015

charged) ODN2395 to bind. We used the crystal structure (Horii et al., 2006) of the GPVI CBD dimer to model ODN2395 interactions (Fig. 2 i). A three-dimensional model of ODN2395 was constructed in a random, linear-like conformation and manually docked into the collagen-binding groove on D1 of a GPVI monomer (Fig. 2 i). A CRP molecule was similarly docked into the groove on D1 (Fig. 2 i), resulting in a CRP-GPVI model consistent with that previously reported (Horii et al., 2006). The linear-like conformation of ODN2395 and CRP have similar diameters (10–12 Å), and the negatively charged PS backbone of ODN2395 was able to interact with the basic (positively charged) residues lining the groove on D1. Approximately nine nucleotides are required to span the D1 groove; thus, a single ODN2395 molecule (22 nucleotides) could interact simultaneously with two GPVI dimers (not depicted). Accordingly, platelet binding and activation was detectable for PS ODN molecules of 18 or more nucleotides; however, smaller PS ODN molecules did not exhibit a significant platelet-activating effect (not depicted). This model of ODN2395-induced clustering of GPVI dimers is analogous to the collagen-induced mechanism of GPVI clustering previously proposed by Horii et al. (2006), which triggers an ITAM-based signaling cascade. Treatment of platelets with 5 μM ODN2395 induced small, albeit physiologically relevant GPVI dimer formation, as detected by increased binding of an anti-GPVI dimer–specific Fab (204-FAB; Jung et al., 2012) by flow cytometry (Fig. 2 j) and by native gel electrophoresis (not depicted). It is likely that oligomeric ODN2395 can interact with and cluster multiple GPVI dimers. Altogether, our observations indicate that the platelet receptor GPVI can bind PS ODNs.

GPVI is the central receptor that mediates platelet–collagen interaction (Nieswandt and Watson, 2003) and plays a crucial role in the recruitment of platelets to the injured arterial wall (Massberg et al., 2003). We therefore used a murine carotid artery ferric chloride injury model to assess potential effects of PS ODNs in vivo. Treatment with ODN2395 but not the nonmodified oligonucleotide significantly reduced occlusion times (Fig. 3 a). Moreover, in a laser-induced mouse mesenteric thrombosis model, discrete tissue injury leads to endothelial cell disruption and collagen exposure. This model is thereby considered to be associated with a prominent role for GPVI in thrombus formation. Significantly larger thrombi were quantified after ODN2395 injection as compared with PBS or nonmodified ODN2395 injection (Fig. 3, c and d). This strongly implies that ODN2395 treatment had accentuated the ability of platelets to form thrombi, possibly by enhancing GPVI responsiveness via clustering/dimerization. Pulmonary embolisms ranging from small asymptomatic to large fatal embolisms are a potential clinical consequence of prothrombotic side effects of drug therapy. Notably, pulmonary thrombus formation could be detected 20 min after i.v. injection of ODN2395 compared with PBS control or nonmodified ODN (Fig. 3 b). These mouse models confirm the relevance of the described platelet-activating effects of ODN2395 in vivo.

Relevance for PS-modified, nucleotide-based therapeutics

Prompted by the observation that the PS backbone modification of TLR9 agonistic ODNs has a major impact on platelet activation, we investigated a range of nucleotide-based therapeutics including oligonucleotides, aptamers, and miRNA mimetics/antagonists. The therapeutic potential of miRNA for multiple diseases has attracted major interest (van Rooij and Olson, 2012). Their inhibition can be achieved by designing antisense oligonucleotides, which directly bind to and inactivate targeted miRNAs (van Rooij and Olson, 2012). PS modifications are used in miRNA therapeutics to achieve protection and stability against proteases and nucleases (Lennox and Behlke, 2011; van Rooij and Olson, 2012). To assess whether miRNA therapeutics can cause platelet activation, platelets were incubated with PS-modified miR-322 and demonstrated significant concentration-dependent binding of PAC-1 (Fig. 3 e), in agreement with a PS backbone but not a specific nucleotide sequence or TLR9 binding causing platelet activation.

Most of the antisense oligonucleotides used in clinical trials carry a PS-modified backbone and reach plasma concentrations approaching 5 μM after i.v. infusion (Chi et al., 2005; Marcucci et al., 2005). The BCL-2–targeting PS-modified oblimersen (G3139) is one of the most widely studied antisense oligonucleotides, which is administered i.v. for the treatment of chronic lymphocytic leukemia (Advani et al., 2011) and melanoma (Ott et al., 2013). We observed significant binding and activation of washed platelets by final concentrations of 50–100 nM G3139 (not depicted), and although G3139 is described to be highly protein-bound (Advani et al., 2011), significant effects on platelets in whole blood assays at input concentrations of 1 μM were observed (Fig. 3, f and g). Although no severe thromboembolic complications have been reported so far with oblimersen, side effects include pyrexia, hypotension, and thrombocytopenia. The reported thrombotic events were classified as catheter-related complications (Advani et al., 2011), possibly related to drug dosing. The maximal plasma concentration of oblimersen, measured after 7 mg/kg continuous i.v. infusion, was 0.84 ± 0.6 μM (Marcucci et al., 2005). Our data show significant effects of ODN2395 in vitro in whole blood assays (Fig. 1 g), as well as assays in vivo in mice treated to attain an ODN2395 plasma concentration of ∼1 μM (Fig. 3 a). Antisense oligonucleotide plasma concentrations vary considerably between patients (Marcucci et al., 2005), implying that plasma concentrations sufficient to cause platelet activation are attainable.

In conclusion, we report a previously unrecognized mechanism of platelet activation mediated through PS backbone modifications of DNA and RNA oligonucleotides. GPVI binds modified oligonucleotides and mediates platelet effects. Sulfur replacements of the nonbinding oxygen have also been identified in some pathogenic bacteria as a postreplicative change (Wang et al., 2007). Thus, our findings may also represent a potential mechanism for platelet activation in bacteremia. As PS modification is a common step in many drug development programs, the described platelet-activating effects

Published February 2, 2015

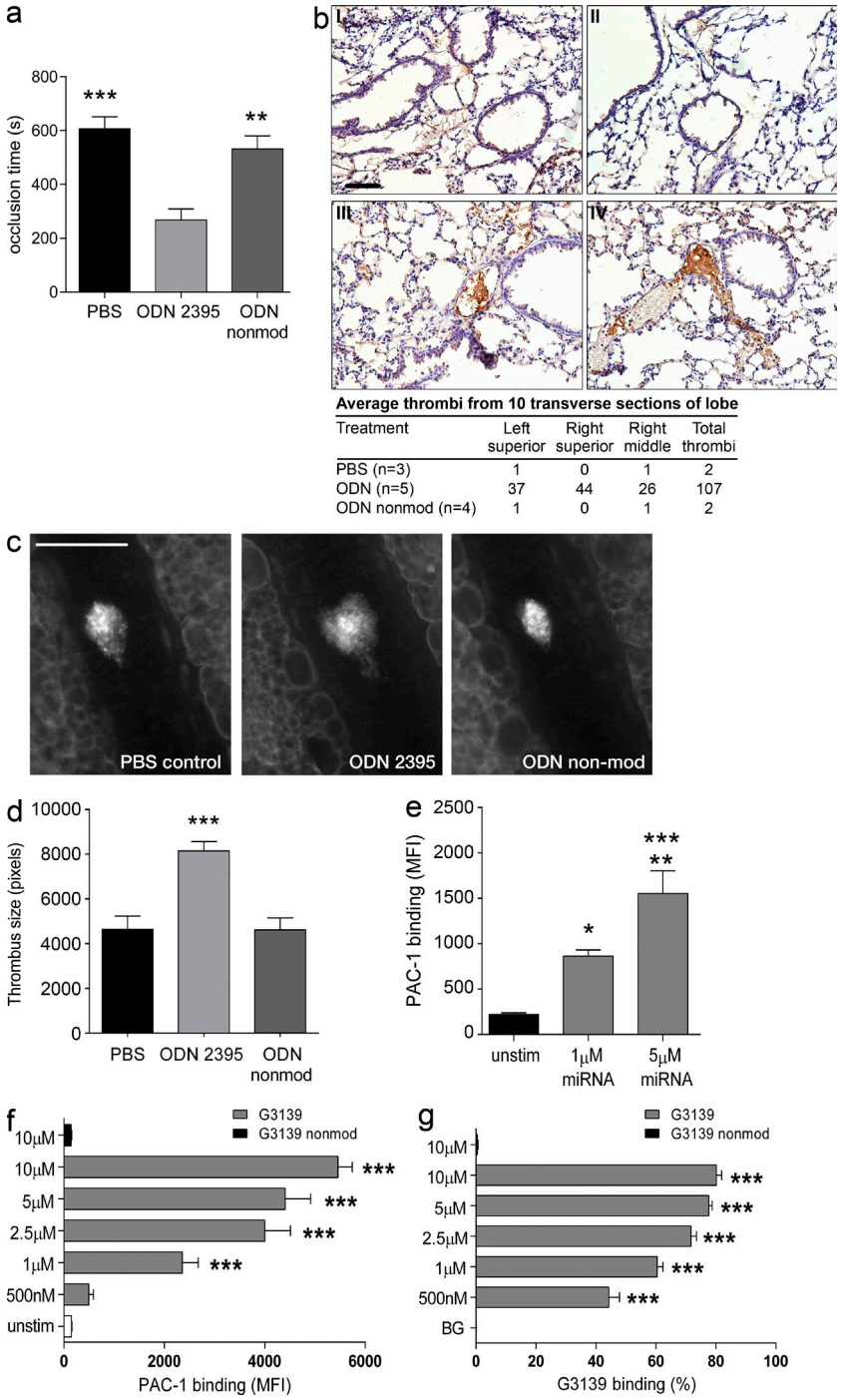

Figure 3. In vivo carotid artery injury, pulmonary thromboembolism, and mesenteric artery injury mouse models; in vitro impact of PS backbone–modified miRNA and antisense oligonucleotide G3139 on platelet activation. (a) Occlusion time after in vivo injection of ODN2395 (0.6 mg/kg body weight) before carotid artery injury compared with PBS control (***, $P < 0.001$; $n = 6$–8) and nonmodified ODN2395 (0.6 mg/kg body weight; **, $P < 0.01$ ODN2395 vs. ODN nonmod; $n = 6$). (b) Thrombus formation in the lung vessels of C57BL/6 mice induced by ODN2395 (1 mg/kg body weight; III and IV); I, PBS injection; II, injection of ODN nonmod (1 mg/kg body weight). Images are representative for four animals/group (control/ODN2395/ODN nonmod). (c and d) Thrombi size in mice injected with ODN2395 (i.v. tail vein injection, 1 mg/kg body weight) compared with PBS injection or ODN nonmod injection, respectively. Original pictures were taken after rhodamine staining (***, $P < 0.001$ vs. PBS and ODN nonmod; $n = 4$–5). (b and c) Bars, 100 µm. (e) PAC-1 binding after treatment with miRNA (miR-322) compared with control untreated samples (*, $P < 0.05$ vs. unstim; **, $P < 0.01$ vs. 1 µM miRNA; ***, $P < 0.001$ vs. unstim; $n = 3$). (f and g) G3139-induced platelet activation and binding in whole blood compared with non–PS-modified G3139 (***, $P < 0.001$ vs. unstim/10 µM G3139 nonmod; $n = 6$). Data are presented as means ± SEM.

should be considered and appropriate hematological tests performed in preclinical and in particular in clinical trials. Our findings support the development and use of alternative chemical modifications to provide nuclease resistance for nucleotide-based therapeutics.

MATERIALS AND METHODS

Antibodies and reagents. FITC-labeled anti-GPIIb/IIIa antibody PAC-1 and PE-labeled anti-CD62P antibody were purchased from BD, FITC-labeled anti-CD61 and APC-labeled anti-CD14 antibody from Beckman Coulter, and streptavidin-PE secondary antibody from Jackson ImmunoResearch Laboratories, Inc. The single-chain antibody (scFv) SCE5 was generated as described previously (Schwarz et al., 2004), and binding was visualized via a Penta-His Alexa Fluor 488–conjugated antibody (QIAGEN). Antibodies against human CLEC-2 were generated as described previously (Gitz et al., 2014). Oligonucleotides ODN2395 (5′-TCGTCGTTTTCGGCGCGCGCCG-3′ with and without PS backbone), FITC-labeled ODN2395 (5′-TCGTCGTTTTCGGCGCGCGCCG-3′ with and without PS backbone), scrambled ODN (5′-TGCTGCTTTTGGGGGGCCCCCC-3′, complete PS backbone), and ODN TTAGGG (TLR9 antagonist, 5′-TTTAGGGTTAGGGTTAGGGTTAGGG-3′, PS backbone) were

Published February 2, 2015

purchased from InvivoGen, biotin-labeled ODNs and G3139 (5′-TCTCC-CAGCGTGCGCCAT-3′, PS backbone) from GeneWorks, and miRNA targeting nucleotides (miR-322, 5′-GGUUUUGUACUUAACGACGAC-3′, PS backbone) from Exiqon. Unless stated otherwise, all other chemicals were obtained from Sigma-Aldrich.

Blood collection from healthy human subjects. Healthy blood donors provided informed consent in accordance with the Declaration of Helsinki. All subjects were free of platelet-affecting drugs for at least 14 d. Blood sampling procedures were approved by the Ethics Committee of the Alfred Hospital, Melbourne, Australia.

Preparation of PRP and washed platelets. Blood was collected by venipuncture with a 21-gauge butterfly needle from healthy volunteers into citrate anticoagulant (Monovette; Sarstedt). PRP was isolated by centrifugation at 180 *g* for 10 min. Washed platelets were prepared from PRP by two additional washing/centrifugation steps (500 *g*, 10 min) in the presence of ACD (acid citrate dextrose) buffer, 0.05 µM PGE_1, and 0.01 U/ml apyrase. The final platelet pellet was resuspended in Tyrode's buffer (137 mmol/liter NaCl, 2.68 mmol/liter KCl, 11 mmol/liter $NaHCO_3$, 10 mM Hepes, 0.42 mM NaH_2PO_4, and 5 mM D-Glucose, pH 7.4) in the same volume as initial PRP and substituted with 1 mM $MgCl_2$ and 2 mM $CaCl_2$ (final concentration).

Pull-down with ODN-coated streptavidin beads. Washed platelets were lysed in lysis buffer (150 mM NaCl, 1% Triton X-100, and 50 mM Tris, pH 8.8) and precleared by incubation with streptavidin beads for 10 min at room temperature (RT); beads coated with either ODN2395-Biotin or ODN nonmod–Biotin (5 µM final concentration) were mixed with cleared platelet lysates for 30 min at RT with rocking. Beads were then pelleted and washed three times with PBS; bead-associated proteins were eluted into 5× Laemmli sample buffer and heated for 5 min at 96°C, then separated by 12% SDS-PAGE and electrotransferred to a polyvinylidene difluoride (PVDF) membrane, and stained with 1 µg/ml anti-GPVI antibody (1G5; Al-Tamimi et al., 2009).

Assessment of ODN2395-mediated tyrosine phosphorylation. Washed platelets were treated with 5 µg/ml CRP-XL, 5 µM ODN2395, or 5 µM nonmodified ODN2395 for 20 min before addition of ice-cold lysis buffer containing 5 mM EGTA, 1% (vol/vol) Triton X-100, 20 mM Tris-HCl, pH 7.4, and complete protease and phosphatase inhibitor cocktail (Roche). Lysates were centrifuged at 1,000 *g* for 5 min, and supernatants were incubated overnight with either 5 µg/ml mouse anti-Src antibody or mouse anti-Syk antibody (GD11 or 4D10.1; EMD Millipore). Src or Syk was then pulled down from the lysates using Protein A–coated beads (GE Healthcare). After washing these beads twice with 0.1% (vol/vol) Tween-20 in PBS, proteins were then eluted by boiling for 10 min in 2× reducing SDS sample loading buffer, and proteins in the eluted fraction were separated by SDS-PAGE followed by electrotransfer to nitrocellulose. Filters were blocked with 20 mM Tris-HCl, pH 7.4, containing 5% (wt/vol) skim milk and then probed with 0.5 µg/ml 4G10 anti-phosphotyrosine antibody (EMD Millipore), 1 µg/ml anti-Src antibody, or 0.5 µg/ml anti-Syk antibody in 20 mM Tris-HCl, pH 7.4, containing 3% (wt/vol) BSA and 0.1% (vol/vol) Tween-20 and visualized using HRP-conjugated anti–mouse IgG antibody and enhanced chemiluminescence (GE Healthcare).

Flow cytometry. To investigate platelet activation, PRP or washed platelets, respectively, were stimulated with oligonucleotides at different concentrations or 20 µM ADP as positive control for 10 min. Thereafter, samples were stained with the appropriate antibodies (PAC-1–FITC and CD62-PE) for 20 min and finally fixed with cell fix (BD). To evaluate platelet-leukocyte aggregates and binding of biotinylated ODNs in whole blood, citrated whole blood was incubated with ODNs (1 µM/5 µM) or ADP (20 µM) for 10 min and stained with the appropriate antibodies. Anti–CD61-FITC was used to define the platelet population, anti–CD14-APC as a monocyte marker, and anti–CD3-PE as a lymphocyte marker. To analyze ODN binding, streptavidin-PE was used for samples preincubated with biotinylated ODN2395. After staining, blood samples were lysed with FACS lysing solution (BD), washed twice, and fixed with cell fix. For whole mouse blood experiments, blood was diluted 1:10 in PBS and stained with the appropriate antibodies, and platelets were gated according to size and positive staining for CD41. 10,000 events in the platelet gate were acquired for each sample. Flow cytometry of lysed blood samples was performed on a FACSCanto (BD), and 2,500 $CD14^+$ events were acquired for each sample to evaluate PMA formation. Analysis was performed using CellQuest Pro for FACSCalibur measures and FACSDiva software for data acquired on FACSCanto (BD). Histogram overlays were generated using FlowJo 7.6.5 software.

96-well plate platelet aggregometry. PRP was obtained as described above, and platelet-poor plasma (PPP) was prepared by centrifugation of PRP (4,000 *g*, 5 min). After 30 min of resting at 37°C, 90 µl PRP was added to wells of a 96-well plate, which were prepared with different concentrations of agonists. The plate was then immediately placed in a 96-well plate reader, and absorbance was determined at 595 nm every 30 s for 60 min between vigorous shaking at 37°C. As reference for maximal and minimal aggregation, PPP and PRP were used, respectively.

Microfluidics assay. Discrete ligand patches were immobilized in microfluidic devices by infusing the ligand solution (100 µg/ml collagen type III and 100 µg/ml fibrinogen) through separate microfluidic "coating" channels. The ligands were allowed to adsorb to the glass surface for 2 h at RT, and unspecific binding sites were blocked by perfusion of 1% BSA. After removal of the coating channels, a second set of microfluidic channels was placed perpendicular to the direction of the first channel. Perfusion of preincubated whole blood samples results in thrombus formation selectively at the discrete coating strips. Vehicle, 5 µM ODN2395, and 5 µM ODN2395 nonmod preincubated samples were perfused for 5 min at a shear rate of 400/s, and formed thrombi were fixed with 1% formaldehyde solution. Flow experiments were performed using an IX81 Olympus microscope, and platelet adhesion was visualized in real time.

Differential interference contrast (DIC) microscopy of adhering platelets. Glass coverslips were coated with 30 µg/ml fibrinogen at 4°C overnight. After washing with PBS, coverslips were blocked with 1% BSA. After adding 5 µM ODN2395 or ODN2395 nonmod, washed platelets were instantly added to the coverslips and incubated for the indicated time points at 37°C. Samples were then washed twice with PBS and fixed with cell fix for 15 min. Finally, DIC (100×) was performed on an Olympus BX61 microscope using an F-View II digital camera.

Intracellular ROS production in platelets. Agonist-induced intracellular ROS production in platelets was quantified by flow cytometry using 2′,7′-dichlorodihydrofluorescein diacetate (H_2DCF-DA) as described previously (Arthur et al., 2012). Dye-loaded platelets were mixed with agonists for up to 20 min and then diluted 10-fold. The stimulation index represents the ratio of mean percentage of events within the gate region (M1) of the resting versus the agonist-treated sample.

Modeling of potential ODN2395 interactions with GPVI. Poisson-Boltzmann electrostatics were calculated for the extracellular GPVI CBD dimer (PDB ID: 2GI7; Horii et al., 2006) using the APBS Tools 2.1 plugin for PyMOL v1.6.0.0 (http://www.pymol.org). CRP (PDB ID: 1CAG) was manually docked into the collagen-binding site on D1 of a GPVI monomer using the collagen-binding residues identified from site-directed mutagenesis experiments (Horii et al., 2006) as a guide. The rigid body docking was performed manually within SYBYL-X 2.1 (Certara, L.P.). The phosphodiester version of ODN2395 (ODN2395 nonmod) was constructed within SYBYL-X 2.1 in a random, linear-like conformation. To obtain the PS-modified version of ODN2395, one of the nonbridging oxygen atoms in each of the 22 nucleotides was replaced with a sulfur atom, and the bond length was adjusted to 1.9 Å; the oxygen replacement was performed in a random manner to obtain

Published February 2, 2015

an oligonucleotide of mixed stereochemistry (i.e., not all Rp or Sp chirality). The PS-ODN2395 was manually docked into the GPVI D1 groove.

Ex vivo and in vivo tests of ODNs in mice. All experiments involving animals were approved by the AMREP animal ethics committee. C57BL/6 mice or TLR9$^{-/-}$ on C57BL/6 background were anaesthetized with 50 mg/kg ketamine and 10 mg/kg xylazine. For ex vivo experiments, the abdominal cavity was opened under deep anesthesia and blood was taken by direct puncture of the inferior caval vein into a tube containing 3.8% sodium citrate.

Carotid artery occlusion time model. The left jugular vein was revealed in male C57BL/6 mice (20–25 g) by an incision to inject reagents. A further incision was made on the right neck to allow careful dissection of the common right carotid artery from its connective tissue. 5 min after the injection of the experimental reagents, a 1 × 5–mm strip of filter paper soaked in 10% ferric-chloride solution was inserted under the vessel for 3 min to cause an injury, which when left untreated will consistently occlude. After 3-min injury, the filter paper was removed, the area was flushed with saline, and a Doppler flow probe (Transonic 0.5 mm) was fitted around the site of injury. Flow speed and time of occlusion were reported.

Laser-induced vessel wall injury in mesenteric arteries. Young male C57BL/6 mice (15–18 g) were chosen to minimize fat surrounding of the vessels. After inferior caval vein injection of 70 µl of 0.05% rhodamine solution and subsequent injection of ODN2395 or ODN2395 nonmod (1 mg/kg body weight) or PBS, the mesentery was exposed. A localized laser injury (440-nm pulsed nitrogen dye laser) was induced to arteries of 70–100 µm in diameter through the objective (20×) of an inverted IX81 microscope (Olympus) with a Micropoint laser system (Photonics Instruments).

Murine pulmonary thromboembolism. Anesthetized male C57BL/6 mice (20–25 g) received i.v. ODN2395 or ODN2395 nonmod (1 mg/kg body weight) or PBS. After 20 min, mice were euthanized and perfusion was performed with 6 ml saline, followed by 6 ml of 10% formalin. Lungs were subsequently removed and fixed for 2 d with 10% neutral-buffered formalin. These organs were then embedded in Tissue-Tek OCT compound (Sakura) and stored at −80°C until use.

Lung cryosections of 8 µm were prepared. After antigen retrieval with 20 µg/ml Proteinase K buffer, thrombi were detected by incubating tissue sections with rat anti–mouse CD41 IgG overnight (clone: MWReg30; AbD Serotec) at 5 µg/ml or saline. Subsequent steps were performed using the Rat IgG VECTASTAIN ABC kit (Vector Laboratories) in which stain was developed using 3,3′-Diaminobenzidine (DAB)–peroxidase substrate. The sections were counterstained with Mayer's hematoxylin and examined using an Olympus BX50 microscope and image captured with MicroPublisher 3.3 RTV digital camera (QIMAGING). For quantification, thrombi of 10 transverse cryosections (200 µm apart) of each lobe (left and right superior and right middle) were counted.

Statistics. Data are presented as means ± SEM and were analyzed using two-tailed Student's *t* test or one-way ANOVA with a Tukey post-hoc test. $P < 0.05$ was considered statistically significant.

This work was supported by the German Research Foundation, a British Heart Foundation Chair account (Prof. Steve Watson), and the National Health and Medical Research Council of Australia.

The authors declare no competing financial interests.

Author contributions: U. Flierl designed and performed experiments, analyzed data, and wrote the manuscript; B. Lim, J.F. Arthur, Y. Yao, and M.T.K. Zaldivia performed experiments and analyzed data; T.L. Nero and M.W. Parker performed analysis of the crystal structure of the GPVI CBD, created docking models, and wrote the manuscript; S.M. Jung, E. Gitz, A. Schäfer, B. Nieswandt, R.K. Andrews, A.Y. Pollitt, M. Jandrot-Perrus, E.E. Gardiner, and K. Peter designed experiments, analyzed data, and wrote the manuscript.

Submitted: 27 February 2014
Accepted: 9 January 2015

REFERENCES

Advani, P.P., A. Paulus, A. Masood, T. Sher, and A. Chanan-Khan. 2011. Pharmacokinetic evaluation of oblimersen sodium for the treatment of chronic lymphocytic leukemia. *Expert Opin. Drug Metab. Toxicol.* 7:765–774. http://dx.doi.org/10.1517/17425255.2011.579105

Al-Tamimi, M., F.T. Mu, J.F. Arthur, Y. Shen, M. Moroi, M.C. Berndt, R.K. Andrews, and E.E. Gardiner. 2009. Anti-glycoprotein VI monoclonal antibodies directly aggregate platelets independently of FcγRIIa and induce GPVI ectodomain shedding. *Platelets.* 20:75–82. http://dx.doi.org/10.1080/09537100802645029

Arthur, J.F., J. Qiao, Y. Shen, A.K. Davis, E. Dunne, M.C. Berndt, E.E. Gardiner, and R.K. Andrews. 2012. ITAM receptor-mediated generation of reactive oxygen species in human platelets occurs via Syk-dependent and Syk-independent pathways. *J. Thromb. Haemost.* 10:1133–1141. http://dx.doi.org/10.1111/j.1538-7836.2012.04734.x

Chi, K.N., E. Eisenhauer, L. Fazli, E.C. Jones, S.L. Goldenberg, J. Powers, D. Tu, and M.E. Gleave. 2005. A phase I pharmacokinetic and pharmacodynamic study of OGX-011, a 2′-methoxyethyl antisense oligonucleotide to clusterin, in patients with localized prostate cancer. *J. Natl. Cancer Inst.* 97:1287–1296. http://dx.doi.org/10.1093/jnci/dji252

Cognasse, F., H. Hamzeh, P. Chavarin, S. Acquart, C. Genin, and O. Garraud. 2005. Evidence of Toll-like receptor molecules on human platelets. *Immunol. Cell Biol.* 83:196–198. http://dx.doi.org/10.1111/j.1440-1711.2005.01314.x

Eckstein, F. 2000. Phosphorothioate oligodeoxynucleotides: what is their origin and what is unique about them? *Antisense Nucleic Acid Drug Dev.* 10:117–121. http://dx.doi.org/10.1089/oli.1.2000.10.117

Eisenhardt, S.U., M. Schwarz, N. Schallner, J. Soosairajah, N. Bassler, D. Huang, C. Bode, and K. Peter. 2007. Generation of activation-specific human anti-$\alpha_M\beta_2$ single-chain antibodies as potential diagnostic tools and therapeutic agents. *Blood.* 109:3521–3528. http://dx.doi.org/10.1182/blood-2006-03-007179

Gibbins, J., J. Asselin, R. Farndale, M. Barnes, C.L. Law, and S.P. Watson. 1996. Tyrosine phosphorylation of the Fc receptor γ-chain in collagen-stimulated platelets. *J. Biol. Chem.* 271:18095–18099. http://dx.doi.org/10.1074/jbc.271.30.18095

Gitz, E., A.Y. Pollitt, J.J. Gitz-Francois, O. Alshehri, J. Mori, S. Montague, G.B. Nash, M.R. Douglas, E.E. Gardiner, R.K. Andrews, et al. 2014. CLEC-2 expression is maintained on activated platelets and on platelet microparticles. *Blood.* 124:2262–2270. http://dx.doi.org/10.1182/blood-2014-05-572818

Grüner, S., M. Prostredna, M. Koch, Y. Miura, V. Schulte, S.M. Jung, M. Moroi, and B. Nieswandt. 2005. Relative antithrombotic effect of soluble GPVI dimer compared with anti-GPVI antibodies in mice. *Blood.* 105:1492–1499. http://dx.doi.org/10.1182/blood-2004-06-2391

Hemmi, H., O. Takeuchi, T. Kawai, T. Kaisho, S. Sato, H. Sanjo, M. Matsumoto, K. Hoshino, H. Wagner, K. Takeda, and S. Akira. 2000. A Toll-like receptor recognizes bacterial DNA. *Nature.* 408:740–745. http://dx.doi.org/10.1038/35047123

Horii, K., M.L. Kahn, and A.B. Herr. 2006. Structural basis for platelet collagen responses by the immune-type receptor glycoprotein VI. *Blood.* 108:936–942. http://dx.doi.org/10.1182/blood-2006-01-010215

Hu, H., P.C. Armstrong, E. Khalil, Y.C. Chen, A. Straub, M. Li, J. Soosairajah, C.E. Hagemeyer, N. Bassler, D. Huang, et al. 2011. GPVI and GPIbα mediate staphylococcal superantigen-like protein 5 (SSL5) induced platelet activation and direct toward glycans as potential inhibitors. *PLoS ONE.* 6:e19190. http://dx.doi.org/10.1371/journal.pone.0019190

Iwasaki, A., and R. Medzhitov. 2004. Toll-like receptor control of the adaptive immune responses. *Nat. Immunol.* 5:987–995. http://dx.doi.org/10.1038/ni1112

Jung, S.M., M. Moroi, K. Soejima, T. Nakagaki, Y. Miura, M.C. Berndt, E.E. Gardiner, J.M. Howes, N. Pugh, D. Bihan, et al. 2012. Constitutive dimerization of glycoprotein VI (GPVI) in resting platelets is essential for binding to collagen and activation in flowing blood. *J. Biol. Chem.* 287:30000–30013. http://dx.doi.org/10.1074/jbc.M112.359125

Krieg, A.M., A.K. Yi, S. Matson, T.J. Waldschmidt, G.A. Bishop, R. Teasdale, G.A. Koretzky, and D.M. Klinman. 1995. CpG motifs in bacterial DNA trigger direct B-cell activation. *Nature.* 374:546–549. http://dx.doi.org/10.1038/374546a0

Published February 2, 2015

Krieg, A.M., P. Guga, and W. Stec. 2003. P-chirality-dependent immune activation by phosphorothioate CpG oligodeoxynucleotides. *Oligonucleotides*. 13:491–499. http://dx.doi.org/10.1089/154545703322860807

Lennox, K.A., and M.A. Behlke. 2011. Chemical modification and design of anti-miRNA oligonucleotides. *Gene Ther.* 18:1111–1120. http://dx.doi.org/10.1038/gt.2011.100

Mangin, P.H., C. Tang, C. Bourdon, S. Loyau, M. Freund, B. Hechler, C. Gachet, and M. Jandrot-Perrus. 2012. A humanized glycoprotein VI (GPVI) mouse model to assess the antithrombotic efficacies of anti-GPVI agents. *J. Pharmacol. Exp. Ther.* 341:156–163. http://dx.doi.org/10.1124/jpet.111.189050

Marcucci, G., W. Stock, G. Dai, R.B. Klisovic, S. Liu, M.I. Klisovic, W. Blum, C. Kefauver, D.A. Sher, M. Green, et al. 2005. Phase I study of oblimersen sodium, an antisense to Bcl-2, in untreated older patients with acute myeloid leukemia: pharmacokinetics, pharmacodynamics, and clinical activity. *J. Clin. Oncol.* 23:3404–3411. http://dx.doi.org/10.1200/JCO.2005.09.118

Massberg, S., M. Gawaz, S. Grüner, V. Schulte, I. Konrad, D. Zohlnhöfer, U. Heinzmann, and B. Nieswandt. 2003. A crucial role of glycoprotein VI for platelet recruitment to the injured arterial wall in vivo. *J. Exp. Med.* 197:41–49. http://dx.doi.org/10.1084/jem.20020945

McKenzie, S.E., S.M. Taylor, P. Malladi, H. Yuhan, D.L. Cassel, P. Chien, E. Schwartz, A.D. Schreiber, S. Surrey, and M.P. Reilly. 1999. The role of the human Fc receptor Fc gamma RIIA in the immune clearance of platelets: a transgenic mouse model. *J. Immunol.* 162:4311–4318.

Nieswandt, B., and S.P. Watson. 2003. Platelet-collagen interaction: is GPVI the central receptor? *Blood*. 102:449–461. http://dx.doi.org/10.1182/blood-2002-12-3882

Ott, P.A., J. Chang, K. Madden, R. Kannan, C. Muren, C. Escano, X. Cheng, Y. Shao, S. Mendoza, A. Gandhi, et al. 2013. Oblimersen in combination with temozolomide and albumin-bound paclitaxel in patients with advanced melanoma: a phase I trial. *Cancer Chemother. Pharmacol.* 71:183–191. http://dx.doi.org/10.1007/s00280-012-1995-7

Schwarz, M., P. Röttgen, Y. Takada, F. Le Gall, S. Knackmuss, N. Bassler, C. Büttner, M. Little, C. Bode, and K. Peter. 2004. Single-chain antibodies for the conformation-specific blockade of activated platelet integrin alphaIIbbeta3 designed by subtractive selection from naive human phage libraries. *FASEB J.* 18:1704–1706. http://dx.doi.org/10.1096/fj.04-1513fje

Semple, J.W., and J. Freedman. 2010. Platelets and innate immunity. *Cell. Mol. Life Sci.* 67:499–511. http://dx.doi.org/10.1007/s00018-009-0205-1

Tapp, L.D., E. Shantsila, B.J. Wrigley, B. Pamukcu, and G.Y. Lip. 2012. The CD14++CD16+ monocyte subset and monocyte-platelet interactions in patients with ST-elevation myocardial infarction. *J. Thromb. Haemost.* 10:1231–1241. http://dx.doi.org/10.1111/j.1538-7836.2011.04603.x

van Rooij, E., and E.N. Olson. 2012. MicroRNA therapeutics for cardiovascular disease: opportunities and obstacles. *Nat. Rev. Drug Discov.* 11:860–872. http://dx.doi.org/10.1038/nrd3864

Wang, L., S. Chen, T. Xu, K. Taghizadeh, J.S. Wishnok, X. Zhou, D. You, Z. Deng, and P.C. Dedon. 2007. Phosphorothioation of DNA in bacteria by dnd genes. *Nat. Chem. Biol.* 3:709–710. http://dx.doi.org/10.1038/nchembio.2007.39